Potential Surfaces and Dynamics: What Clusters Tell Us

R. Stephen Berry

Department of Chemistry and The James Franck Institute, The University of Chicago, Chicago, Illinois 60637

Received February 16, 1993 (Revised Manuscript Received July 6, 1993)

Contents

I. Introduction 2379
II. Mapping the Landscape 2380
A. The Benchmarks: Methods and Characteristics 2380
B. The Landscapes: Small Systems 2383
1. The Approaches 2383
2. Homogeneous Clusters of Atoms 2384
3. Binary Systems: The Alkali Halides 2386
4. Effects of Anisotropy 2386
5. Potential Surfaces for Small Molecular Clusters 2387
C. The Landscapes: Larger Systems 2387
1. Clusters of Atoms and Atomic Ions 2388
2. Large Molecular Clusters 2389
III. Eroding and Building the Landscape 2390
A. Small Systems 2390
B. Large Systems: Glass Formation 2392
IV. Closing Remarks 2393
Acknowledgments 2393
References 2393

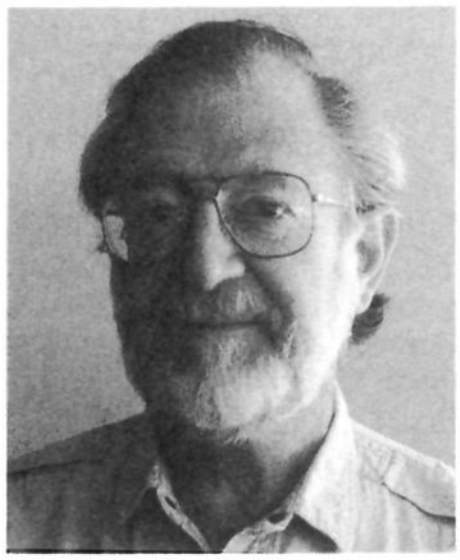

R. Stephen Berry, a Colorado native, received his degrees from Harvard and taught at The University of Michigan and Yale before joining The University of Chicago in 1964. He has been a visiting professor at The University of Copenhagen, The Université de Paris-Sud, and Oxford. His current interests, in addition to multidimensional potential surfaces and clusters, include dynamics of other few-body systems such as electron correlation in atoms, atomic and molecular collisions, finite-time thermodynamics, and energy and resource policy.

I. Introduction

This is a review of work dealing with the landscapes of multidimensional potential surfaces and with the dynamics determined by those surfaces. The varieties of methods for constructing such surfaces from first principles or from spectroscopic and other empirical data are not included here;[1-3] neither is a collection of references to the potential surfaces that have been constructed for triatomic and other polyatomic molecules,[4] or a review of the analytic representation of potential surfaces.[5] In fact we begin with the assumption that we have in hand a prescription for the surface we want to study. From there, this discussion concentrates on these aspects of the potential surfaces of polyatomic molecules and clusters: (a) how to find important regions, particularly stationary points, on multidimensional potential surfaces if an analytic or numerical representation of the surface is known (strictly, there can be isolated nonanalytic points on the surface[6]); (b) how the shape of the landscape depends on elementary characteristics of the parameters of the potential, such as the range of the pairwise interactions and the strengths of polarizabilities; (c) how the shape of the multidimensional landscape can be distorted in systematic ways by varying parameters of elementary interactions; and (d) how certain dynamical properties, notably the glass-forming or crystal-forming capacity, are consequences of the geography of the potential surface.

This arrangement of topics gives structure to the discussion: the first describes methods for finding important characteristics of surfaces, notably minima and saddles and densities of locally stable equilibrium states. This section also addresses statistical sampling methods for finding densities of equilibrium states for systems of many particles, for which complete determination of all the local minima would be out of the realm of possibility, and raises some of the open questions about important information regarding potential surfaces that we do not yet know how to obtain. It also discusses briefly ways of putting to diagnostic use the methods of exploring multidimensional surfaces. The next part of the paper concerns the explorations of how the landscape of a multidimensional potential surface depends on simple, particle–particle interactions and how the variation of parameters in the elementary interactions can be used to tune and vary the shape of a multidimensional potential, at least in model calculations and simulations. The last part of the paper addresses the relation between the landscape and certain aspects of the dynamics on that landscape; what kinds of minima and saddles must a surface have if the system is to exhibit a liquidlike form? What are the characteristics of a surface that assure that a finite system, annealed from a nonrigid or liquid condition, will find its global minimum—or, alternatively, will be likely to find itself trapped in a high-energy minimum, for example a disordered geometry? While complete coverage of these dynamic properties would require a substantial review of its own, this discussion strives to give some introduction to the subject and a doorway to its rapidly expanding literature. Topics such as the chaotic and regular behavior of several-particle systems,

0009-2665/93/0793-2379$12.00/0

Table I. The Number $g(N)$ of Geometrically Distinct Isomers of Clusters of Atoms Bound by Pairwise, Isotropic Lennard-Jones and Morse Potentials, as a Function of the Number N of Atoms in the Cluster[a]

N	6	7	8	9	10	11	12	13
$g(N)_{L\text{-}J}$	2	4	8	18	57	145	366	988
$g(N)_{Morse}$[b]	1	3	5	8	16	24	22	36
$g(N)_{Morse}$[c]		4	9					

[a] For the former, the parameters do not affect the shape of the landscape, only its scale. For the Morse potential, the parameters are chosen to simulate clusters of argon atoms. [b] From ref 12. [c] From ref 133.

the transition between them, and their connection to the shape of the potential surface have not been addressed here. Neither has the special topic of potential surfaces of polymers, bio and otherwise; this can be thought of as the subject of potential surfaces discussed here, but with the added constraints that the only allowed motions are those that preserve the chemical bonds of the system and, thereby, the backbone structure of the polymer. One of the tantalizing, open issues central to this topic is finding how much we learn about potential surfaces from clusters and simple molecules can be transferred and applied in the context of polymers. Last among the neglected topics is a comparison of quantum and classical characteristics. This is involves (a) the question of validity of the adiabatic or Born–Oppenheimer approximation and of the representation of the dynamics of a system with a single potential surface, and (b) the degree to which densities of quantum states and densities of classical states give rise to significantly different observable behavior. Regarding the properties directly relevant to the topics of this paper, we can make this generalization: clusters of helium atoms and hydrogen molecules behave quite differently from their classical counterparts, qualitatively so; clusters of neon have quantum effects large enough to make their behavior quantitatively different from their classical analogues but qualitatively similar, and clusters of argon atoms have quantum effects small enough that their behavior is well described by classical mechanics, even well down into the temperature or energy range in which they are solidlike.[7]

Potential surfaces of three-body systems are simple and well-studied, at least by comparison with the potential surfaces of four-particle and larger systems.[5] These can now be studied in as much detail as one might wish. By contrast, here we are concerned primarily (but not exclusively) with the potential surfaces of systems consisting of at least six and as many as a few hundred particles. These systems may be conventional molecules, which normally exhibit only one or perhaps a very few stable geometries, or they may be clusters of atoms, molecules, or ions that, like bulk condensed matter, may be found in any of a large number of locally stable geometric structures. The number of these structures depends sensitively on the number of atoms or molecules in the system. Table I gives some exemplary values of the number $g(N)$ of geometrically distinct, locally stable structures that have been found for clusters of atoms bound by pairwise, isotropic Lennard-Jones and Morse potentials, for clusters composed of 6 to 13 particles. This number appears to increase exponentially with N. However the number of minima on the surface, $\xi(N)$, is of course far larger than $g(N)$ because each geometric structure appears on the surface with many permutations of its identical atoms. For example the four stable structures of the 7-particle Lennard-Jones cluster in order of increasing energy, the pentagonal bipyramid, the singly-capped octahedron, the triply-capped tetrahedron, and the skew, doubly-capped trigonal bipyramid, have 504, 1680, 1680, and 5040 permutational isomers, respectively. The singly-capped pentagonal bipyramid, the lowest-energy structure of the 8-particle Lennard-Jones cluster, has 40 320 permutational isomers. Roughly, the number of permutational isomers increases factorially with N. Hence the N-dependence of $\xi(N)$ is approximately $N!\exp(aN)$, a function that grows at a frightful rate.

This rapid growth with N has an important implication: it means that, while it may be possible to catalog and map a complete potential energy surface for a cluster of as many as 6 or 7 or possibly 9 or 10 atoms, it makes no sense at all to try to map in full the potential surface for a system of 15, 20, or more atoms. The amount of information is simply greater than we could wish to manipulate. This means that the study of multidimensional potential surfaces for systems of more than three internal degrees of freedom breaks naturally into two or three categories: at one extreme is the study of systems small enough that it is feasible to catalog all the minima and the important saddles that connect them, and the geometry and topology of the surface, both how the geometrically different stable structures are linked and how the geometrically equivalent but permutationally different sets of locally stable structures are connected. Next is the study of potential surfaces that can be modeled and explored fairly extensively so that their densities of locally stable states can be assessed with considerable reliability by statistical searches. Finally there are the forms of bulk matter, for which the few stable crystalline geometries are relevant to all but amorphous or glassy materials, and for these, sampling can only give a qualitative sense of what kinds of specific geometries may occur, and a quantitative sense of such properties as the extent of long-range and short-range order.

II. Mapping the Landscape

A. The Benchmarks: Methods and Characteristics

The first step toward elucidating the structure of a multidimensional potential surface is to decide what can be learned about it and what would be worth knowing. We are concerned with intramolecular reactions (isomerizations), and perhaps with intermolecular reactions as well, and are not confining ourselves to regions immediately surrounding the global minima and the spectroscopic properties of systems in those regions. In fact one of our considerations later in this section is the testing and evaluation of the extendability to entire surfaces of potentials developed for limited, spectroscopically probed regions close to global minima. What, then, is important and what is possible to find?

The most obvious characteristics of any potential surface are its minima. For small systems, it has proven relatively simple to find global minima, even all the

geometrically distinct local minima, for surfaces given by pairwise potentials, for molecules and clusters of as many as 13 particles (see Table I). However the numbers in Table I for the larger systems may be only lower bounds; it is not absolutely certain that all the minima of the 12-particle Lennard-Jones or Morse cluster have been found; the numbers are the result of search procedures which do not necessarily find all the stable structures. Hoare and Pal, for example, originally used a growth algorithm, which does not find stable structures that enter newly at some N and that have no precursors for smaller N.[8-12] Later work of theirs used more than one growth algorithm. Growth algorithms involve adding one new particle to a presumably stable site on a known, stable N-particle structure; the energy of the $(N+1)$-particle cluster is then minimized to allow small adjustments of the structure. Typically, the new particle is put onto a site of maximum possible coordination number in the search for each new stable structure.

A common method now for finding minima from classical mechanics is the combination of simulation by a molecular dynamics (MD) or Monte Carlo (MC) method combined with quenching, as used by Stillinger and Weber:[13] at an arbitrary point in the simulation, the kinetic energy is set to zero and the system is taken down as direct a path as possible to the local minimum around which the system had been moving at the moment the kinetic energy was set to zero. Two methods have been used frequently to reach the local minimum, the method of steepest descents and the conjugate gradient method. The method of steepest descents[14,15] moves each coordinate q_i in the time step τ according to the equation

$$\frac{dq_i}{d\tau} = -\frac{1}{m_i}\nabla_i V(\mathbf{q}) \qquad (1)$$

which takes the representative point of the system downward but at a rate that decreases as the gradient decreases. A faster way to find minima is the conjugate gradient method, in which, after each move or a short series of moves, the next step is made orthogonal to the one before.[16,17]

Still another method has recently been put forward, based on powerful methods of optimization theory.[18] If the potential can be transformed to be the difference of convex functions, then bounds can be computed by a relatively efficient algorithm on the energy of the global minimum. The method was illustrated with clusters of 3–24 identical atoms bound by traditional pairwise Lennard-Jones potentials.

Finding minima is now very straightforward, except insofar as there is no guarantee that any of the methods just described will find the global minimum structure. This is not a problem for small clusters, but can be for moderately large clusters or molecules. For example such searches might well not find the global minimum for something like $(NaCl)_{40}$ or $(CaO)_{36}$. However the geometries of "magic number" systems, with their convincing, closed-shell structures, are now usually easy to find: the 55-particle Lennard-Jones cluster might have as its lowest-energy structure an icosahedron, a face-centered cubic cubooctahedral or a hexagonal close-packed structure. The first is in fact the global minimum and the cubooctahedron is a saddle for this particular system.[17] It was rather a surprise when, in 1972, Hoare and Pal found that the most stable structure for the 13-particle Lennard-Jones cluster is a regular icosahedron and that the face-centered cubic cubooctahedron is a saddle and not a minimum.[19,20] An interesting recent development was the search for local and global minima of medium-sized water clusters[21,22] by Tsai and Jordan. Starting with a variety of intuitively-chosen structures and a semiempirical potential, they found many local minima, mostly based on fused cubic structures and, presumably, global minima among them. The energies of the structures were then checked with ab initio calculations in the vicinity of the minima. As the authors point out, the semiempirical potential may exaggerate the stability of the fused cubic structures over ring or fused-ring structures, and that optimizations based on the ab initio calculations would now be in order.

The second characteristics of the potential surface to find are the saddle points. We discuss here the two most widely used methods that have evolved to do this; there have been several others that might well deserve further exploration.[23-29] All of these were developed in the context of isomerization of conventional molecules and hence of potential surfaces that presumably can only be developed reliably from many solutions of a Born–Oppenheimer Schrödinger equation. They therefore arose from a viewpoint that knowledge about the potential is going to be somewhat limited, just because of the cost of finding an adequate number of points in all regions of a multidimensional space. Sometimes saddles and the shapes of surfaces near saddles are inferred from experimental data; an example is the cyclobutene–butadiene surface.[30] The dynamical and kinetic aspects of classical and quantum passage from one minimum to another over a saddle form a very extensive subject which has been reviewed very thoroughly[31] and will not be explored here.

The most extensively studied and almost the oldest method to find saddles is a "hill-climbing" method.[32-39] In this approach, the search starts at or very near a minimum of the potential, where a normal mode is selected. This mode is followed upward, with regular corrections to take into account the evolving apparent force constant. The gradient and Hessian must be evaluated at nearly every step, a task that can be done efficiently by numerical evaluation. The Cerjan–Miller version was made into a fast, practical algorithm, capable of handling rather large clusters,[40] and was then applied more systematically to Lennard-Jones clusters of 55 atoms[41] and then to clusters as large as 150 atoms.[17]

The second approach to finding saddles that has been used for global searches is a skiing-down method,[42] the method of "slowest slides." This is a useful complement to the hill-climbing methods because the latter, while they essentially always find saddles, do not necessarily find all the saddles and can sometimes miss very important saddles, particularly if they are not dominated by any single normal mode of vibration. In this method, one begins with a molecular dynamics or Monte Carlo simulation, and finds, by tracking, a region of maximum potential energy through which the system passes. The simulation is halted in the vicinity of the potential maximum, the kinetic energy is removed, and a steepest-descent trajectory is begun. The rate of

descent is usually fast at first, then slows to a very low rate as the saddle is approached and then accelerates as the system moves away from the saddle, as it starts it downward trajectory toward the next minimum. The point of minimum rate of descent is presumably about as close to the saddle as any point along that descent path. The quality of that point as an approximation to the saddle can be estimated from the values of the derivatives of the potential there. One can then iterate to find a better approximation, until one is satisfied that the first derivatives are as near zero as one desires. In practice, two iterations have been quite adequate to locate saddles this way, even on surfaces for 50 or 60 particles.

The method of "slowest slides" is slower than the hill-climbing method, by a factor of about 3–8. However "slowest slides" finds saddles that (a) are important, as evidenced by their appearance in molecular dynamics simulations and (b) may be overlooked by the hill-climbing procedure, particularly if they are well off any normal mode direction. A good practice turns out to use both methods—hill climbing to find most of the saddles and slowest slides to find any other important saddles missed by the hill-climbing search. A still better, faster procedure makes use of the slowest-slides method to find the vicinity of the saddle and the nearby minimum below it, and then switches to eigenvector following in order to locate the saddle precisely.[43]

There are other characteristics of multidimensional potential surfaces that are worth knowing, some of which can be obtained by available methods and others which we do not yet know how to find. In the first category are the eigenvalues of the Hessian matrix, $\{\partial V(q_i,q_j)/\partial q_i \partial q_j\}$, the set of second derivatives of the potential, at the important stationary points. At minima, these tell us which directions to take in implementing the hill-climbing method; every positive eigenvalue of the Hessian at a minimum is the force constant of a normal mode of vibration for that basin. At saddles, the number of negative eigenvalues is the number of independent directions in which the curvature of the surface is negative, the number of coordinates along which the system can slide to lower energies; i.e. that number is the rank of the saddle.

It was believed for many years that the lowest saddle between any two minima must be of rank 1, that is, that any saddle along the (lowest-energy) reaction path connecting any two minima must be a simple saddle, with only one direction of negative curvature.[44] However it turns out that the conditions for the validity of this statement, the Murrell-Laidler theorem, are more stringent than need be for real molecules, so that saddles along reaction paths may in fact connect more than two minima.[6] This makes it interesting in some cases to determine the ranks of saddles along reaction paths.

One other kind of information contained in the eigenvalues, notably the positive eigenvalues, of the Hessian at a saddle is the extent to which a saddle opens above the saddle point. Large positive eigenvalues imply steeply rising walls and narrow canyons above the saddle, and consequently constricted passages that transmit only very well-aimed trajectories; small positive eignevalues imply open passageways and channels across passes that are easy to find, and hence large transmission coefficients. This characteristic of multidimensional potentials has not yet been given as much attention as it probably deserves. Still one more characteristic of the region near a saddle has proven useful. This is a measure of the flatness of a simple saddle, $(\omega_1^2)^{1/2}$, the root-mean-square of the one negative frequency averaged over a segment of trajectory that spans the length of the saddle region. This has been used recently as an index of how much the saddle region contributes to the chaotic character of a trajectory.[43]

Another kind of information about a multidimensional potential which remains to be gathered is the multidimensional counterpart of the area of a lake. The hyperarea $\mathcal{A}(E)$ of the connected region at energy E, or, more strictly, $k_B \ln[\mathcal{A}(E)]$, is the *microcanonical entropy* of the system at that energy. In other words, $\mathcal{A}(E)$ is the measure of configuration space available to the system at energy E and hence its logarithm is the configurational entropy of the system at constant energy, in contrast to the more common $S(T)$, the corresponding entropy of an isothermal system. It seems beyond reach at present to find $\mathcal{A}(E)$ accurately for arbitrary energies. However it is entirely feasible to find a discrete set of points on the perimeter of the lake, simply by using the hill-climbing algorithm to go up along all the local normal coordinates until the desired energy E' is reached. The set of configurations at E' define the desired points. The next step, yet to be implemented, is the estimation of the hyperarea from the finite set of points. This can be done in any of several, successively more complicated but more accurate ways.[45] The simplest is the encompassing sphere method, in which the hyperarea is the hyperarea of the smallest hypersphere that encloses all the points. The next method in order of complexity is the convex hull method,[46,47] based on building an approximate volume from a set of simplexes. The most complex is the α-shape method, while allows for concave as well as convex regions.[48] This method has not yet been implemented, it seems, for systems of more than three dimensions. The questions to ask are (a) how different are the results from the three methods and (b) how much difference to be microcanonical entropy do the differences in the estimated volumes make? These will presumably be addressed relatively soon.

One other aspect of potential surfaces that we can investigate, at least for moderately small systems, is the topology of the surface. What are the connecting paths between particular minima? How are permutationally different, geometrically identical stable structures linked by reaction paths? How do higher-energy minima link with each other and with more stable minima? The potential surface of the trigonal bipyramid, for example, has 20 geometrically and energetically equivalent minima, each of which is joined to three others by a pseudorotation path, so that the totality of the pathways forms a picture of the connectivity of this surface. We shall give an illustration of the topology of a surface that can be derived from scrutinizing its geometry, but we shall not go into the general topological problems such as bounding the numbers of saddles; topologies of potential surfaces have attracted interest and can be related to the forms of the splittings of sets of near-degenerate states and spectral lines.[31,49,50]

B. The Landscapes: Small Systems

1. The Approaches

Mapping the landscapes of multidimensional potentials breaks naturally into two classes of exploration. One is the mapping of relatively simple surfaces, for systems with as many as 15 or perhaps 30 degrees of freedom, for which it is possible to find all the minima, the important saddles that link them and the pattern of connectivity among permutationally different but geometrically equivalent regions; the other is the class of surfaces of larger systems, that can only be studied in statistical terms. From a different perspective, there are at least two uses to which such explorations can be put, particularly explorations of small systems. If the potential surface is fairly reliable, as is the Lennard-Jones or Aziz potential[51-53] for rare gas clusters and the Born–Mayer[54,55] or Born–Mayer–plus-polarization[56,57] potentials for alkali halide clusters, then the surface derived from that potential can be used for interpreting spectroscopic and dynamic properties of the system. If, on the other hand, the potential is known to be reliable in only a restricted part of the configuration space of the system, as in situations in which a potential is derived from spectroscopic data obtained near one or two minima of the surface, then exploration of the full surface can be used to diagnose its global reliability and to determine the regions of configuration space for which the potential must be refined.[58] Here, we shall concentrate on surveying what has been learned from reliable or, at least plausible potentials, and merely give an example to illustrate the exploration of surfaces for purposes of refinement, a topic that is still very much in its infancy.

Hoare and Pal made the first extensive compilations of the minima of rare gas clusters bound by pairwise Lennard-Jones and Morse potentials.[8-12] Since then, minima have been cataloged for many other clusters, including more rare gas clusters,[17,59] molecular van der Waals clusters,[60] alkali halides,[56,57,61] simple metals,[62] transition metals[63,64] and semiconductors,[65-67] as well as some clusters containing dopant or impurity species.[68] (These citations are mostly reviews; specific examples are noted below, in their appropriate contexts.)

Finding saddles has proved to be a considerably greater challenge than finding minima. In many contexts, finding saddles has been intimately linked to finding "reaction paths"—paths of minimum energy connecting two minima. Selected saddles became the objectives of some of the earliest search methods, such as the saddles located by combining semiempirical quantum calculations of the effective, Born–Oppenheimer potentials, their gradients, and Hessian matrices in the vicinity of saddles. This was carried out in the pioneering studies of McIver and Komornicki when they examined the isomerizations between cyclobutene and butadiene[23] and between hexatriene and cyclohexadiene.[25] However their methods were not applicable to the task of finding and cataloging many saddles; they required that one know roughly where to look before one started to search. Even now, for molecules and clusters that cannot be described reliably by interatomic or interionic effective potentials, molecules and clusters that require new solutions of the electronic, Born–Oppenheimer Schrödinger equation at each new nuclear configuration, finding and cataloging saddles is still restricted to only identification of the few that can either be found easily by the hill-climbing method or be located by knowledge or intuition of approximately what the reaction path of interest must be. For example locating the saddle along the path between acetylene, HC≡CH, and ethylidene, $H_2C{=}C$, was one of the frequent tests of new methods.[27,33,37,69] Here we are concerned with methods for and results from global searches, at least to the extent they can now be executed; one hope of course is that methods now applicable to rare gas clusters and alkali halide polymers will become applicable to polyatomic molecules of all sorts.

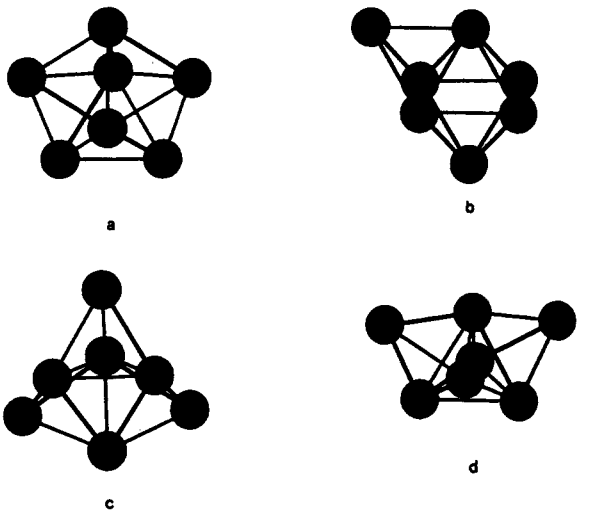

Figure 1. The four stable structures of Ar_7, as well as of seven particles bound by pairwise Lennard-Jones potentials or by Morse potentials having the same curvature at the potential minimum as that of the Lennard-Jones potential: (a) the pentagonal bipyramid, $E = -0.2758 \times 10^{-12}$ erg; (b) the capped octahedron, $E = -0.2663 \times 10^{-12}$ erg; (c) the tricapped tetrahedron, $E = -0.2606 \times 10^{-12}$ erg; (d) the bicapped trigonal bipyramid, $E = -0.2596 \times 10^{-12}$ erg, with Lennard-Jones parameters of $\sigma = 3.4$Å and $\epsilon = 1.671 \times 10^{-14}$ erg.

Extensive but crude mapping of potential surfaces, particularly finding the energies and structures at both minima and the saddles that connect them, was the next natural step after the mapping of minima alone, as done so extensively by Hoare and Pal. This was carried out by the method of slowest slides,[42] the hill-climbing method,[40] and then a combination of the two methods[58] for a number of illustrative systems. These include several that we would call "small" in the context of the nomenclature used here—the minima can all be located and the important saddles that connect them, possibly others as well, can also be found. The "small systems" were Ar_7, Ar_8, $(KCl)_4$, formaldehyde H_2CO, and seven Be^+ ions in a trap. The previously known four minima of Ar_7 and seven of the eight minima of Ar_8 were studied in these and one closely related subsequent investigation.[59] An illustration is shown in Figure 1, the locally stable structures of Ar_7, Figure 2, eight of the saddle structures of Ar_7, and Figure 3, a schematic cross section of the potential surface of Ar_7 showing the energies of the structures of Figures 1 and 2 and how they are linked.

The connections between the stable structures of Figure 3 almost all follow one of two kinds of paths over their saddles. The most common and generally the kind that has the lowest energy at its saddle is the

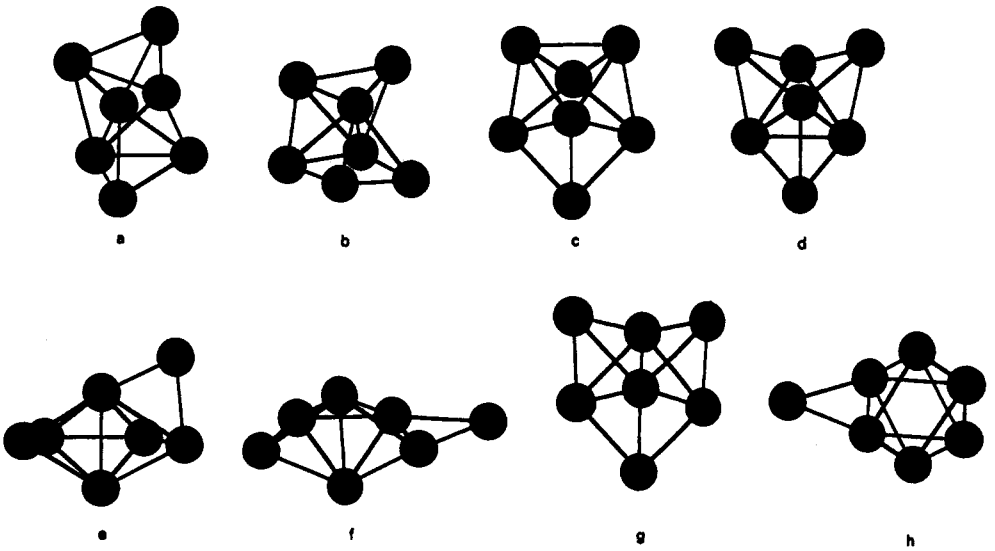

Figure 2. Eight of the saddle structures of Ar_7, making links between the stable structures of Figure 1 as follows: (a) between b and d by a single diamond–square–diamond (DSD) process, $E = -0.2554 \times 10^{-12}$ erg; (b) between a and d by a single DSD process, $E = -0.2511 \times 10^{-12}$ erg; (c) between a and b by a single DSD path, $E = -0.2581 \times 10^{-12}$ erg; (d) between b and c by a single DSD path, $E = -0.2560 \times 10^{-12}$ erg; (e) between a and d by a (high-energy) edge-bridging path, $E = -0.2439 \times 10^{-12}$ erg; (f) between two structures of type c by an edge-bridging path, $E = -0.2431 \times 10^{-12}$ erg; (g) between a and c by a more complex path, $E = -0.2512 \times 10^{-12}$ erg; (h) between two structures of type b, capped octahedra by edge-bridging, $E = -0.2523 \times 10^{-12}$ erg.

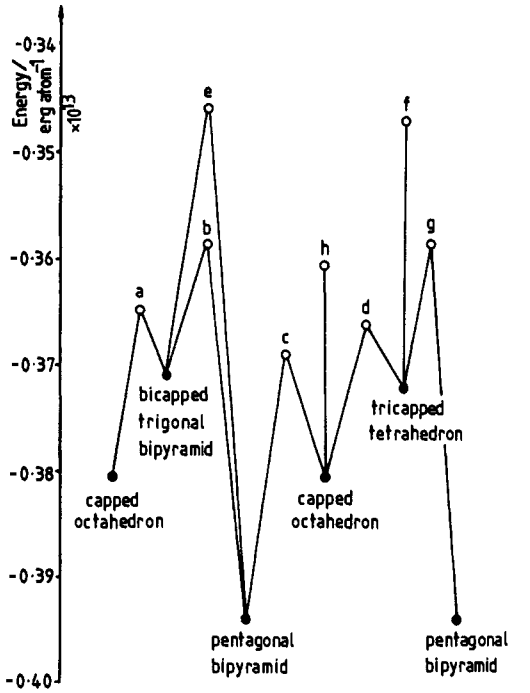

Figure 3. A schematic cross section of the energy surface of Ar_7, showing the minima of Figure 1 (filled circles) and the saddles of Figure 2 (open circles, denoted by the letter labels used in Figure 2).

"diamond–square–diamond" or DSD process, in which two triangular faces with a common edge distort until all four outer edges of the figure are equivalent (the saddle structure) and then continue until a new shared edge is formed, perpendicular to the first. This process is shown in Figure 4a. The second most important process seems to be the edge-bridging process in which a particle leaves one face and goes to an adjacent face by bridging an edge along the way, as shown in Figure 4b.[70] The reason the edge-bridging saddles are generally higher in energy than the DSD saddles is easy to see: in the DSD process, a new bond is forming while an old

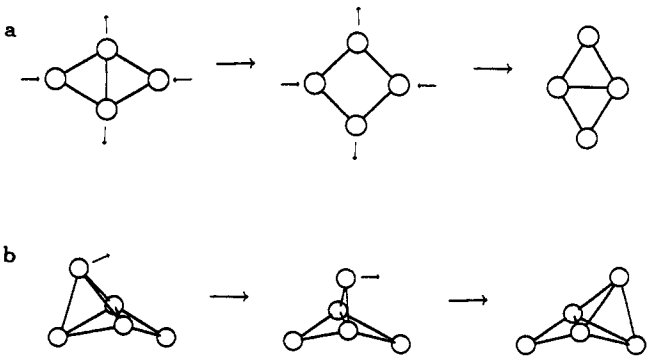

Figure 4. The two of apparently commonest rearrangement processes, schematically: (a) the diamond–square–diamond process; (b) the edge-bridging process.

bond is breaking, but in the edge-bridging process, one nearest-neighbor interaction is essentially completely lost before another can form. Moreover in a simple edge-bridging process, the moving atom has, at most, three bonds and loses one of these along the reaction path; in a DSD process, the participating atoms may all have more than three bonds.

2. Homogeneous Clusters of Atoms

It is instructive to examine the geometries and topologies of simple, Lennard-Jones clusters at this point. The corresponding six-atom cluster, which we can represent as LJ_6 or Ar_6, has a regular octahedron (OCT) as its lowest-energy structure and a distorted octahedron as its one other kind of minimum, a structure specified more precisely by the name "incomplete pentagonal bipyramid" (IPB), because of its close resemblance to a pentagonal bipyramid with one equatorial atom missing. These are shown in Figure 5. The same structures occur for metal atoms modeled by a Gupta potential.[71] The distortion that connects these stable structures can be considered as a DSD process

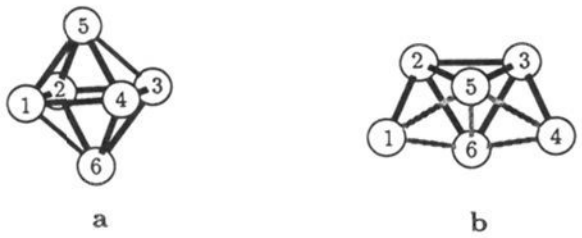

Figure 5. The two stable structures of Ar_6 or the Lennard-Jones cluster LJ_6: (a) the lowest-energy structure, a regular octahedron (OCT); (b) the higher-energy incomplete pentagonal bipyramid (IPB).

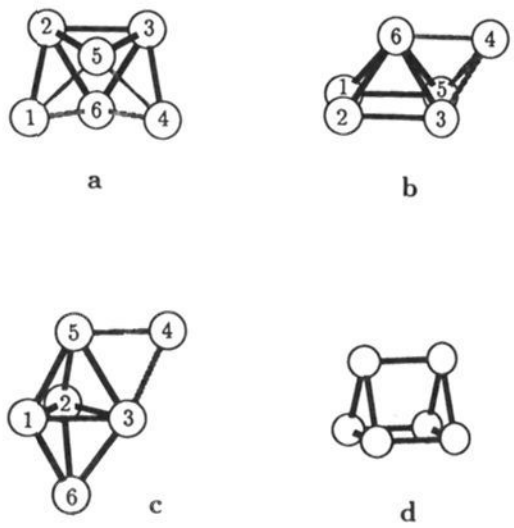

Figure 6. The structures of the Ar_6 or the Lennard-Jones cluster LJ_6 at the four kinds of saddles on its potential surface: (a) the incomplete pentagonal bipyramid, IPB(1), that links the stable octahedral and IPB structures; (b) the capped, square-based pyramid, CSBP(1), that links two stable IPB(0)'s; (c) the edge-bridged trigonal bipyramid, EBTP(1); (d) the trigonal prism TP(3) which, for Ar_6, is a third-order saddle, i.e. has two negative force constants and links three independent downward-sloping paths.

in which a bond on an edge of the octahedron is broken and is replaced by a bond between the polar atoms of the IPB. The potential surface of this LJ_6 cluster has four saddles, shown in Figure 6. One, the trigonal prism, is a second-rank or third-order saddle on the Lennard-Jones surface (but see below concerning other surfaces). The lowest-energy saddle of this system is an incomplete pentagonal bipyramid much like the higher-energy minimum, and links the octahedron with its distorted IPB; each of the 30 geometrically equivalent but permutationally distinct octahedra is connected this way to 12 geometrically equivalent IPB's, so the surface has 30 "clocks", each with a deep well in its center and 12 shallower wells around it. Each of these 12 locally-stable IPB's is connected not only with its "home" octahedron; it is also connected with other IPB's, each in a set that surrounds a permutationally different octahedron; the connecting path goes via a simple saddle that we can call either a capped, square-based pyramid (CSBP) or a slewed trigonal prism. The process that takes an IPB to a different IPB through a CSBP is itself a DSD pathway, in which one of the four equivalent bonds is replaced by a new bond across the (nonpolar) quadrilateral that bond bisects. There are therefore four pathways from each stable IPB to other IPB's in other "clocks". The fourth kind of saddle is an edge-bridged trigonal bipyramid and occurs at an energy higher than the other two simple saddles. All these structures are enumerated in Table II.

A systematic method for extracting the connectivity and the molecular symmetry group has been developed which enables one to choose the molecular symmetry group appropriate to the extent of the configuration

Table II. Stable Structures and Saddles for the Six-Particle Lennard-Jones, Rare Gas, or Gupts Cluster[a]

(a) The Minima

structure (order)	point group	number	connectivity
OCT(0)	O_h	30	12 to IBP's 8 to OCT's
IPB(0)	C_{2v}	360	1 to OCT's, 4 to IPB's

(b) The Saddles

structure (order)	point group	number	pathway
IPB(1)	C_{2v}	360	OCT(0)–IPB(0)
CSBP(1)	C_s	720	IPB(0)–IPB(0)
EBTB(1)	C_s	720	OCT(0)–OCT(0) or IPB(0)–IPB(0)
TP(3)	D_{3h}	120	OCT(0)–OCT(0)

[a] From ref 133.

space that the molecule or cluster can explore with whatever internal energy it has. In this six-atom system, there might seem to be three regions of energy relevant to the molecular symmetry group. In the lowest range, the system is restricted to its octahedral minimum-energy geometry and the symmetry group is O_h, the octahedral group. In the second range, the system can occupy the distorted IPB structures with their C_{2v} symmetry, but if one of these is accessible, then 12 equivalent structures of this geometry are all equally accessible, and must be occupied with equal likelihood. Hence the average symmetry remains O_h so long as the cluster cannot leave the vicinity of its original octahedron, and the molecular symmetry group is the same as that in the low-energy range. In the third range, the system can explore the paths between IPB's around permutationally different octahedra, and can reach all of the 30 "clocks". Consequently in the third region, the appropriate molecular symmetry group is the full rotation–permutation group.

One of the curious aspects of multidimensional potential surfaces is the nature of the boundaries separating different catchment basins. Intuition based on a surface in a three-dimensional space is likely to be quite misleading here. This is because the boundaries of the catchment basins on such a conventional, smooth surface, a function of two independent variables, are smooth curves, the ridge lines. In a space with only one more independent variable, the boundaries of the catchment basins are fractal in one set of coordinates, but in another are smooth.[73] The example used for this study was the three-atom cluster, which has stationary points on its potential surface at the equilateral triangle and the three linear configurations, and, with suitable anisotropic interactions, at three isosceles-triangular geometries as well. The points on the surface can be assigned and correspondingly colored according to what stationary point is reached by a numerical search procedure starting at that point, in the manner of Richter and Peitgen.[74] If the pair interactions are taken to be Lennard-Jones, the minimum is the equilateral triangle and the linear configurations are saddles; with Wales' choice of anisotropic interactions, the linear configurations are minima, the equilateral triangle is a second-order saddle and there are three first-order saddles at isosceles configurations. The hill-climbing procedure (or eigenvector-following procedure, as it is also called) converges for all the initial points chosen,

in contrast to the much better known Newton–Raphson procedure which gave convergence problems.[72]

3. Binary Systems: The Alkali Halides

Alkali halide clusters or polymers are extremely attractive subjects because they offer opportunities for both reliable modeling and experimental study. The models treat the atomic components as spherical ions with exponentially repulsive cores (Born–Mayer model, usually with the parameters ρ and A_{ij} given the values of Tosi and Fumi[55]). The pair potential between any two ions with charges q_i and q_j separated by the distance r_{ij} is, with no polarization

$$V(r_{ij}) = q_i q_j / r_{ij} + A_{ij} \exp(-r_{ij}/\rho)$$

Mutual polarization of the ions can also be incorporated.[54] The stable structures of the alkali halide polymers and their vibrational spectra were investigated extensively by Martin and co-workers.[61,75–80] One of the points especially relevant here is the recognition that the most stable structure may depend on the energy or temperature of the cluster.[78] The tetramer of NaCl, $(NaCl)_4$, has a cubic, rocksalt-like lowest-energy structure, but the free energy of the planar ring becomes lower than that of the cube at temperatures above about 500 K. Phillips, Conover, and Bloomfield[81] determined the structures of the five or six lowest-energy stable forms of $(NaCl)_n$ clusters, $2 \leq n \leq 15$, and of the singly-charged clusters $(NaCl)_nNa^+$ and $(NaCl)_nCl^-$, $2 \leq n \leq 14$.

Alkali halides have been used to study the robustness of interferences about stable structures with respect to variations in the potential surface. Models for ionic clusters always raise questions regarding the importance of polarizabilities. Welch et al.[56,57] and then Diefenbach and Martin[80] examined this issue and found that inclusion of realistic polarizabilities charges the binding energies and equilibrium distances and changes the geometries of a few of the stable structures. Here are three examples: $(CsI)_3$ is predicted to be a planar rectangle when polarizabilities are included but a planar hexagon when the ions are rigid and unpolarizable. The structures predicted for $(CsF)_{11}$ and $(CsF)_{13}$ with and without polarization of the ions are altogether different: without, rocksalt-like but with, layered hexagons. However the geometries of the stablest structures depend rather sensitively on the parameters of the Born–Mayer potential, as reflected by the differences in structures shown by different alkali halides.

An illustration of the mapping of the potential surface of a binary system is the set of five minima on the potential of (KCl_4) and the saddles between them.[82] These are shown in Figures 7 and 8. The same kind of analysis was applied to $(KCl)_5$, which exhibits at least 15 minima and 17 saddles. (Both of these were done with no polarization in the potentials.)

4. Effects of Anisotropy

The structures of clusters of anisotropic species have also been studied. Inclusion of realistic three-body terms has little effect on the total binding energies of simulated argon clusters.[83] The addition of polarization forces to Born–Mayer models of alkali halides was mentioned previously; an analogue for homogeneous

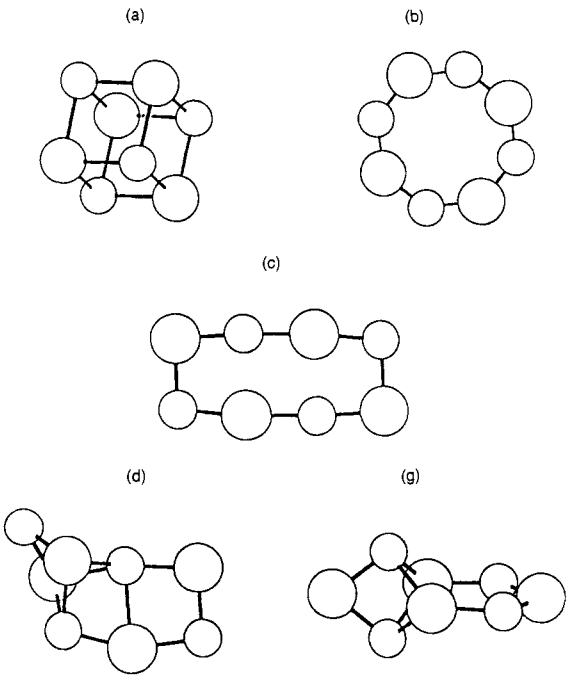

Figure 7. The four most stable geometric structures of $(KCl)_4$ and one other of the group of four, nearly-degenerate locally stable structures, labeled to correspond to the structures in Figure 8: (a) the rocksalt-like, most stable state, $E = -3.1209$ eV per ion; (b) the octagon, $E = -3.0656$ eV per ion; (c) the rectangle or "ladder", $E = -3.0615$ eV per ion; (d) a distorted rectangle, $E = -3.0136$ eV per ion; (g) a distorted octagon, $E = -3.0129$ eV per ion. Taken from ref 82.

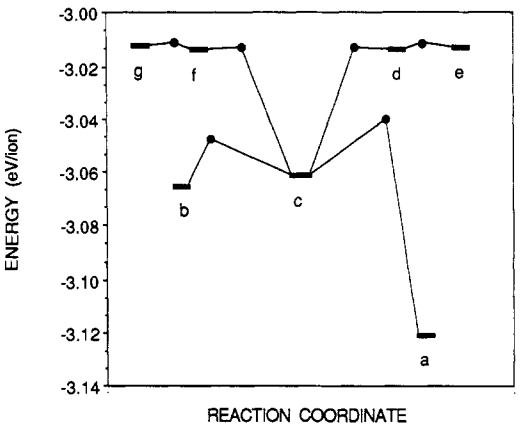

Figure 8. A schematic representation of the cross section of the potential energy surface of $(KCl)_4$, showing the energy levels of the five structures of Figure 7 and two others that are nearly degenerate with the highest two shown in that figure. Taken from ref 82.

atomic clusters is the inclusion of induced dipole-induced dipole forces as in the Axilrod–Teller three-body potential, which has been studied by Wales[84] and then by Doye and Wales.[85] With realistic parameters, the most important effect of the three-body terms is a change in the sequence of some of the excited-state minima, and for the six-particle cluster studied by Doye and Wales, an elaboration of the surface and the variety of minima, saddles, and rearrangement processes. In contrast to the six-particle Lennard-Jones cluster, the six-particle Axilrod–Teller cluster may exhibit up to 44 minima, of which 26 are planar, and at least 75 saddles. The six-particle system was studied as a function of the value of the coefficient specifying the strength of the anisotropic potential; not all these

minima and saddles occur for the weaker range of the strength parameter.

Another much-studied atomic cluster system for which many potentials have been developed is that of silicon; Wales and Waterworth[67] give references to the sources for these potentials. The most recent, whose authors Li, Johnston, and Murrell (LJM) tried specifically to avoid recognized shortcomings of many of its other semiempirical predecessors, was studied by its developers[86] and then in more detail.[67] This potential contains three-body terms, including terms as high as quartic in the interparticle distances. The results from these explorations were compared with a variety of earlier calculations, particularly ab initio attacks.[87-96] The results apparently are not yet in satisfactory agreement with ab initio calculations, particularly of close-packed structures. However most of the results of simulations of silicon clusters, of both structures and reaction paths, are still untested by experiment.

Potential surfaces of covalently bonded molecules are considerably more difficult to construct than the surfaces of most of the clusters that have been modeled until now, comparable in difficulty to semiconductor clusters except insofar as clusters of materials such as silicon and germanium are homogeneous. We shall not discuss the empirical methods of "molecular mechanics" at all, and mention only examples to indicate the direction this subject is taking. The most effective approach seems to be to use a Hartree–Fock, self-consistent field calculation, guided by chemical intuition, to locate approximately the minima, important saddles, and reaction paths, and then to follow this with a more accurate but considerably more costly calculation that includes effects of electron correlation. For reactions and potential surfaces of unsaturated hydrocarbons, the Hartree–Fock method generally locates stable geometries of molecules with reasonable reliability, even though it is not very reliable for finding vibration frequencies or dissociation energies. In cases of symmetry-allowed reactions, the geometries of saddles found this way seem plausible,[97] but of course it is rare that the structure of a transition state can be determined experimentally. An interesting illustration is the surface of the 16-atom system consisting of two cyclobutadiene molecules, in the region that governs their dimerization.[98] The reaction occurs as a Diels–Alder process, with a double bond of one cyclobutadiene adding to the two double bonds of the other cyclobutadiene. In the laboratory, the dominant product has one ring adding over the other (syn configuration) although the calculations of Li and Houk indicate that the more stable product has a "*Z*" or anti configuration. The interpretation of this result is that the saddle point of the reaction path from two cyclobutadienes to the syn product has an energy lower than that of the transition state for formation of the anti structure. At this saddle, the incipient dimer has the structure of a square, right prism. The symmetry of this transition state makes it a case that exemplifies the violation[6] of the Murrell–Laidler rule[44] that saddles corresponding to transition states should have only one negative force constant, i.e. should link the catchment basins of only two stable structures. Since there are four ways to make the U-shaped syn dimer from the transition state, the saddle there must link four equivalent catchment basins. The potential surface of this system has another set of saddles on the way down from the dimerization saddle toward the stable syn minima; these correspond to degenerate Cope rearrangements in which a syn structure passes from one structure to another, equivalent structure by opening of the two bonds holding the original two rings together and forming a new bond between two previously distant carbon atoms.

5. Potential Surfaces for Small Molecular Clusters

A few clusters consisting of a single molecule in a shell of rare gas atoms have been simulated or studied analytically, primarily with the goal of interpreting spectra of the molecule which was introduced as a chromophoric probe. The most important information to emerge from these studies that pertains directly to this review is that there are apparently two types of stable structures for such systems as SF_6 with Ar_N[99,100] which had been studied experimentally through the infrared spectrum of the SF_6,[101] and benzene with Ar_N[68,102-104] studied through the electronic spectrum of the benzene.[105] In both of these systems, one stable form has the molecule surrounded by argon atoms and the other has the molecule on the surface of the cluster. Reaction paths and saddles for such clusters have not yet been studied.

Molecular clusters display arrays of minima and saddles considerably richer than those of atoms, as we would expect from the anisotropy of most molecular potentials. Apart from structural studies of van der Waals dimers and a few trimers and water clusters, studies of structures and potential surfaces of molecular clusters have dealt with large systems, so we reserve the further discussion of this topic for section C, below. The exploration of potential surfaces of molecular clusters is in fact a topic ripe for investigation now. The problems are considerable because, even if the component molecules are considered rigid, the three orientational degrees of freedom add to the three translational degrees so that while a 13-atom cluster is still marginally a small cluster, a 13-molecule cluster is complex enough to have to be treated as a medium-sized system, whose energy landscape we cannot expect to map completely.

C. The Landscapes: Larger Systems

While it is possible to map the minima, saddles, and even reaction paths for clusters and molecules consisting of five or 10 atoms, it is neither practical nor desirable to carry out anything like a complete mapping for a cluster or molecule composed of, say 50 atoms. The first task in dealing with such a problem is deciding what information is worth having, that is, in choosing what questions to ask. Getting systematic catalogs of detailed topologies is possible in principle, perhaps, for as many as 50 atoms, but seems an unjustifiable, costly task. However it is worthwhile to have an estimate of the densities of configurational states, from which thermodynamic properties and a considerable body of kinetic information can be assembled. Constructing such densities is now an entirely feasible task that can be carried out by a combination of analytic methods, computational sampling and curve-fitting. It now seems worthwhile also to begin to study densities of saddles,

but this task has not yet been carried out for medium-size or large clusters or molecules.

1. Clusters of Atoms and Atomic Ions

The approaches to extracting information about the potential surfaces of large clusters have all had their roots in simulation. Some treatments have focused on distinguishing one crystal form from another and predicting what structure a cluster would assume.[106] Others have been oriented less toward structures per se and more toward the dynamics of large systems. While early molecular dynamics simulations concentrated on phenomena such as phase changes, Stillinger and Weber showed that many liquid systems spend much of their time vibrating in potential wells surrounding very regular, low-energy structures.[15,107] The method for finding the "significant structures" is a kind of instantaneous cooling, a mathematical quenching of the species being simulated. During a molecular dynamics simulation, the mechanical motion is stopped at an arbitrary instant, the kinetic energy of the cluster or molecule is set to zero with the system in its configuration kept in its instantaneous configuration. Then the system is taken downhill by any of the standard methods such as steepest descents or conjugate gradient, mentioned earlier, until the system reaches the bottom of its catchment basin. The energy and configuration of the system are the automatic products of the procedure. By carrying out many such quenches, Stillinger and Weber showed that some liquidlike systems, such as two-dimensional Lennard-Jones clusters of 256 particles (with periodic boundary conditions) with enough energy to be liquidlike, spend a very large fraction of time oscillating around minima corresponding to very regular geometries, almost perfect crystallike structures in most cases.

Another way to deal with large clusters was the method developed by Labastie and Whetten[108] for evaluating densities of states. They pointed out that the canonical distribution at each temperature T reflects the density of states with a Boltzmann weight factor. By constructing the distributions of occupancy of each energy band for just a few temperatures, specifically by constructing these in histogram form, they were able to extract the density of states as a function of the total energy of the cluster. This distribution includes both the configurational and vibrational energy. It could, in principle, be done by considering the canonical distribution as a Laplace transform of the density of states, and then carrying out an analytical (or numerical) inverse Laplace transform, as can be done to extract cross sections from rate coefficients;[109] this approach has not yet been exploited to derive densities of states of medium-sized systems.

The next stage in the analysis of medium-sized and large systems was the combination of Stillinger and Weber's quenching, Stillinger's separation of the lowest-energy catchment basin from the partition function,[110] and Bixon and Jortner's separate treatment of the vibrational partition function of that lowest-energy basin[111] and Labastie and Whetten's sampling procedure[108] together with an approximate way to evaluate the vibrational factors of the partition function to derive the density of *configurational* states.[112] This method was carried out with $(KCl)_{32}$ as the exemplary system,

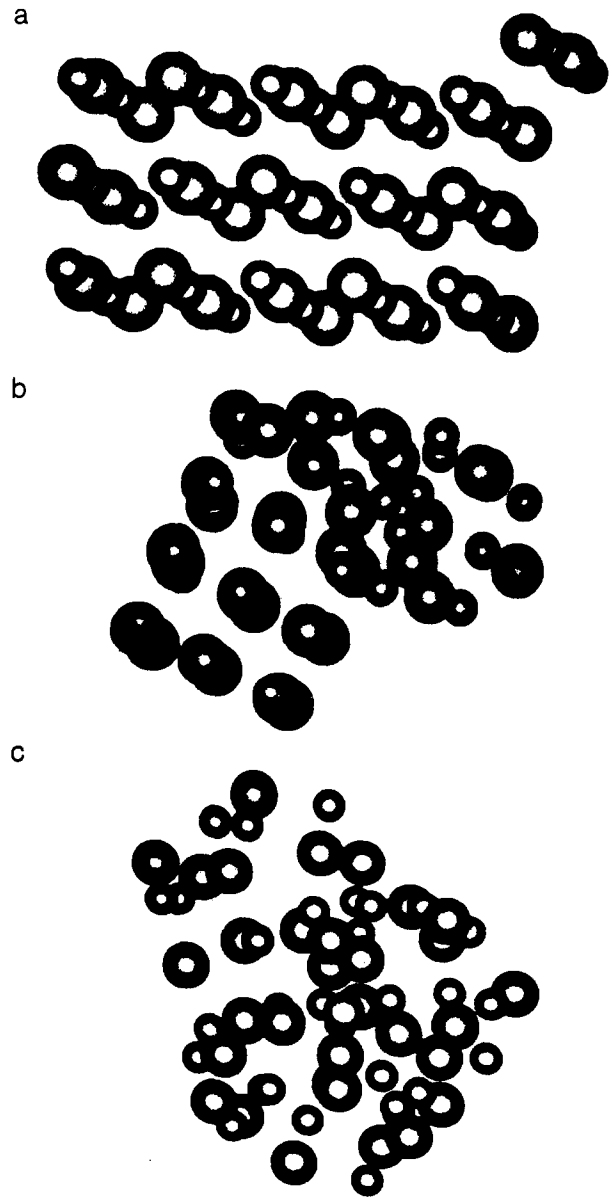

Figure 9. The structures of three kinds of configurations of $(KCl)_{32}$: (a) the first excited configuration of $(KCl)_{32}$, (b) a typical "nonwetting" structure, and (c) a typical amorphous or disordered structure. Taken from ref 112.

clearly too large to analyze fully but small enough to tempt one to try to do better than to treat it as if it were a sample of bulk matter. In the fact the quenching "experiments" with this species showed that the configurational states can be classified into four categories. The first is the single $4 \times 4 \times 4$ rocksalt cube whose energy of −3.3703 eV per ion is the global minimum of the configurational energy of this "magic number" cluster. The next in energy is a group of states in a narrow energy band beginning about 0.017 eV per ion higher, all of which are like bits of slightly defective rocksalt crystal; the lowest-energy configuration in this band has the structure shown in Figure 9a. The next energy band, overlapping the defective rocksalt structures a little, from about −3.34 eV per ion to about −3.31 eV per ion, arises from an unusual set of structures that arise only because molten alkali halides, both bulk and clusters, do not wet their solid counterparts;[112-114] these structures are characterized by being regular and rocksalt-like on one side and very disordered on the

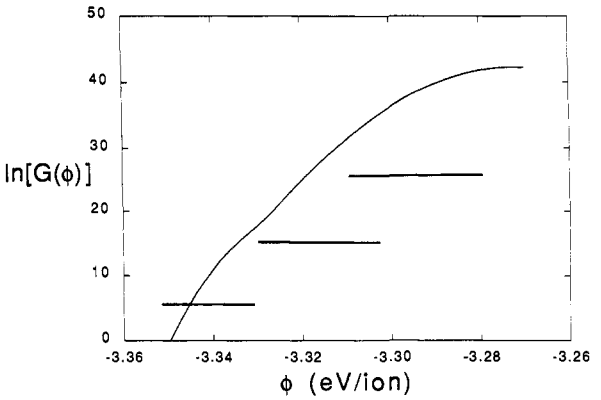

Figure 10. The density of configurational states of $(KCl)_{32}$. Modified from ref 116 to show the ranges of the three bands of states: defective crystal-like, nonwetting, and amorphous.

other. We have called them "nonwetting" structures. Overlapping the upper two-thirds of the nonwetting range, from just below −3.315 to almost −3.295 eV per ion, where evaporation becomes significant, is the band of amorphous or disordered configurations. Although precisely these four categories can hardly be expected to be universal, we may expect that more "normal" medium-sized and large clusters, whose melts wet the solidlike form, will exhibit locally stable forms of three kinds: (a) a lowest-energy configuration, (b) slightly defective configurations very much like that of the lowest-energy structure, and (c) amorphous or disordered structures. Defective, nearly regular structures are known, for example for Ar_{13} and Ar_{55}, which have one atom removed from the outer shell of the icosahedral ground states and placed on the center of one of the triangular faces.

We should not expect to find a counterpart of the nonwetting structures that arises from clusters with melted surfaces because, although clusters of about 50 or more atoms are expected to show a state in which their surfaces are liquid and their cores are solid, the configurations at the bottoms of the catchment basins in which these molten-surface clusters exist correspond to regular polyhedra with a few atoms promoted out of the surface layer so that, given enough energy, the promoted atoms can "float" around the cluster's surface.[115] However this is just conjecture at this time and needs to be investigated for clusters of arbitrary size.

The density of locally stable configurational states of a cluster as large as $(KCl)_{32}$ grows enormously, as Figure 10 shows. The density of amorphous structures dominates the total density at all energies where amorphous structures exist; there are at least 10^{10} times as many potential minima associated with amorphous structures as there are minima associated with nearly-regular, defective rocksalt-like structures. This is apparent when quenching is done from an initial state with energy high enough to make the amorphous structures accessible, essentially meaning that the initial state must be a fully molten state. Virtually every quench takes the system to an amorphous structure; a few take it to a "nonmelting" structure. However if the $(KCl)_{32}$ system is brought to a local minimum by a systematic energy reduction procedure, even as fast as 10^{12} K/s if expressed in equivalent temperature terms, the cluster finds its way to either the global minimum $4 \times 4 \times 4$ cube or to one of the slightly defective rocksalt structures.[116] Only by shortening the range of the long-range Coulomb interaction to a much attenuated, shielded Debye or Yukawa potential can the potential surface develop deep enough high-energy wells to trap amorphous clusters when the cooling rate is in the conceivably attainable range of 10^{11} to 10^{12} K/s.[116] This kind of distortion will be discussed in the final section, section III.

2. Large Molecular Clusters

Considerable experimental information is available that is relevant to the shapes of the potential surfaces of some large systems, for example the observation, by electron diffraction, of liquid and plastic rhombohedral forms of carbon tetrachloride by the same technique.[117] Electron diffraction of clusters has largely been much more successful with large than with small clusters. Homogeneous clusters of simple chlorohydrocarbons and of SeF_6 studied this way[118,119] display various solidlike phases corresponding to different minima on their potential surfaces. It has proved possible in some cases to distinguish experimentally between minima whose connecting reaction path involves translational motions of the molecules and minima, whose connecting path is primarily a reorientation of the molecules of the cluster, and to find at least three packing arrangements of the molecules.[20]

Simulations of molecular clusters, particularly of such pseudospherical molecules as CCl_4[121] and TeF_6,[122] have been carried out primarily to investigate phase changes in these clusters, but they nevertheless reveal some of the characteristics of the multidimensional potential surfaces. Bulk tellurium hexafluoride exhibits a bcc plastically crystalline form just below its freezing point, as do the hexafluorides of S, Se, and transition metals. At lower temperatures the hexafluorides of S, Se, and large clusters, but not bulk TeF_6, become monoclinic and then, at very low temperatures, TeF_6 clusters regain symmetry and become orthorhombic. Transition metal hexafluorides do not exhibit an intermediate monoclinic form, transforming simply to orthorhombic at low temperatures. Simulations used to interpret this behavior of TeF_6 were done with seven-center Lennard-Jones interactions between the atoms of 250 (and, for comparison, of 54 and 128) rigid, octahedral molecules of TeF_6, and both Monte Carlo and molecular dynamics simulations were used. The transitions the 250-atom clusters showed were monoclinic-to-bcc on heating and the reverse on cooling, over the temperature range 90–110 K (on cooling) and 90–140 (on heating). Whether the width of this range is due to relaxation and hysteresis, or to the finite temperature range over which finite systems can exhibit coexistence[123,124] could not be determined. A monoclinic cluster of 128 atoms, heated, began its tranformation to bcc at about 75 K, as expected of the smaller cluster. An orthorhombic cluster of 128 molecules, undergoing heating, transformed directly in the range 90 to 135 K, to bcc without passing through a monoclinic form. From this information, we can infer that the barrier, at least the free-energy barrier, between orthorhombic and bcc is higher than the monoclinic-to-bcc barrier but lower than the orthorhombic-to-monoclinic. This is consistent with the facile mechanism proposed by Raynerd et al.[125] and by Pawley and Dove.[126] Bartell and Xu make the point

that if the hexafluorides were spherical, the monoclinic structure would "transform smoothly to body-centered cubic" but the orthorhombic would become hexagonal close packed and that passage between the monoclinic–bcc part of the potential surface and the orthorhombic–hcp part requires considerable structural reorganization. The treatment of this system illustrates state-of-the-art analysis of the very complex potential surfaces of moderately large but finite molecular aggregates.

III. Eroding and Building the Landscape

The power of simulation extends well beyond representing real systems at arbitrary levels of accuracy. One of the tools it offers in the study of multidimensional potentials is the capacity to vary and tune the shape of the potential surface in a systematic way. Some examples of the more straightforward ways this can be used were cited earlier, in the content of noncentral and multibody interactions. A more far-reaching aspect of such tuning is the variation of the basic pair interactions of the component particles of the molecule or cluster, particularly of the long-range part of the potential. The reason is that the long-range, centrosymmetric part of the pair potential has a very strong influence on the number and shape of the high-energy minima of the multidimensional potential surface. In other words, by varying parameters of the pair potential, one can deform the multidimensional potential and control the shapes and numbers of the catchment basins. More specifically, the longer the range of the attractive forces between pairs of particles is, the fewer minima and catchment basins there are, and the larger the mouths of the deepest catchment basins become.

Two lines of interest led to the investigation of deformation of multidimensional surfaces. Stillinger and Weber[127] and then Stillinger and Stillinger[128] approached the subject from the viewpoint of nonlinear optimization, initially as a potential alternative to simulated annealing[129] for broad classes of optimization problems. The other was aimed specifically at studying the shapes of multidimensional landscapes.[130–133] Deliberate, controlled deformation of such landscapes quickly suggests itself as an attack on the protein-folding problem,[134] for example. The method has also been used to study the conditions for glass formation.[116]

Stillinger and Stillinger[128] tuned the parameters of the pair interaction by generalizing the Lennard-Jones potential, of form Ar^{-12}–Br^{-6}, to $A^{(n)}r^{-2n}$–$B^{(n)}r^{-n}$, with n a variable. Braier et al. used a Morse potential and varied the scale factor of the exponential. Both potentials are of the form $V(r) = \epsilon[[g(r) - 1]^2 - 1]$ with the well depth or dissociation energy ϵ, and the function $g(r) = (r_0/r)^n$ for the generalized Lennard-Jones case and $g(r) = \exp[-\beta(r - r_0)]$ for the Morse potential. Variation of the extended Lennard-Jones potential has not yet been explored deeply, but it is clear from the study of the 13-particle cluster that extending the range by reducing n increases the probability that a randomly chosen configuration of the cluster will lie in the catchment basin of the icosahedral global minimum-energy structure. Piela et al.[130–132] smoothed their surfaces by finding points of inflection around local maxima and successively reducing the height of the local bumps. No comparison of modifications based on this method with the other methods have yet been made.

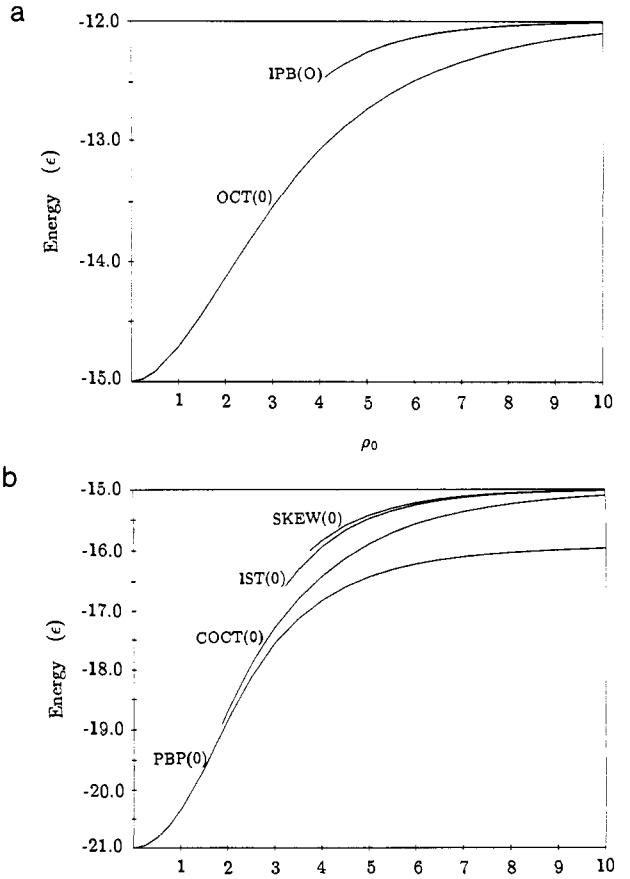

Figure 11. The energies of the local minima of the clusters M_6 (a) and M_7 (b) as functions of the range parameter ρ_0 of the Morse potential. Note that each of the higher minima exists only for values of ρ_0 above its own critical minimum value, e.g. $\rho_0 = 4.10$ for the higher-energy structure of M_6.

A. Small Systems

The effects of changing the range of the Morse potential on the shape of the potential have been studied in some detail. Six- and seven-particle clusters, designated M_6 and M_7, were used by Braier et al. for this purpose.[133] The range parameter can be put into scaled form, as $\rho_0 = \beta r_0$. If the potential curves of a variety of known, chemically-bound homonuclear diatomic molecules, including rare gas dimers, some transition metal dimers, and the weakly bound alkaline earth dimers, are fit to Morse curves, their scaled range parameters ρ_0 fall between 2 and 7. If $\rho_0 = 6$, the curvature of the potential at its minimum is the same as that of the Lennard-Jones potential; the structural and dynamic properties of simulated Morse ($\rho_0 = 6$) and Lennard-Jones clusters are almost identical. The M_6 and LJ_6 clusters have the same two kinds of stable structures (Figure 5) and the M_7 and LJ_7 clusters likewise both have the same four stable structures shown in Figure 1, when $\rho_0 = 6$. However if ρ_0 is reduced, making the range of the pair attraction longer, the higher-energy wells become shallower and then disappear. Figure 11 shows the energies of the stable minima of M_6 and M_7 as functions of ρ_0. Each of the higher minima exists only for ρ_0 greater than some critical value; if we think of the minima in the parameter space of ρ_0, each of the critical values corresponds to a fold catastrophe on the energy surface. Figure 12 illustrates this with three cuts through the potential surface, one

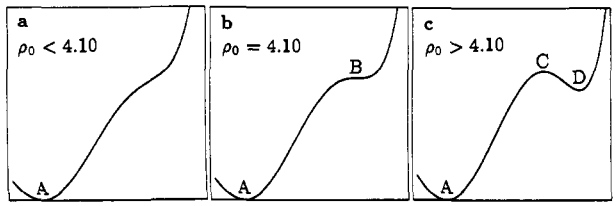

Figure 12. A schematic representation of three cuts through the potential surface of M_6, corresponding to values $\rho_0 < 4.10$, $\rho_0 = 4.10$, and $\rho_0 > 4.10$, i.e. to the surface that cannot support a secondary minimum, to the critical value of the range for that minimum, and to a surface whose value of ρ_0 is high enough to support the secondary minimum of M_6.

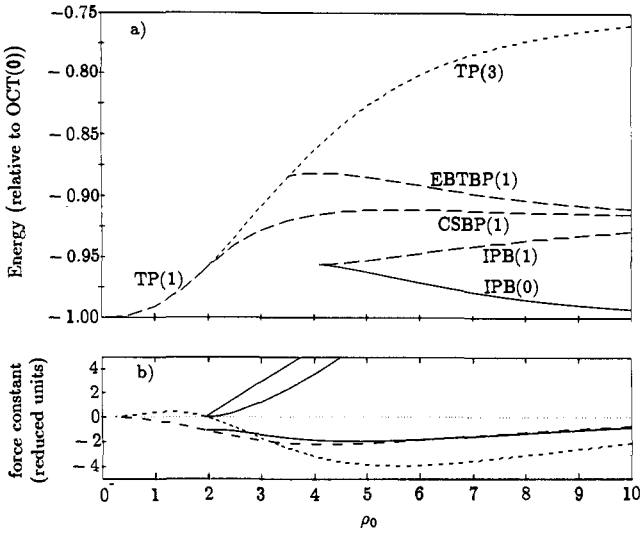

Figure 13. The energies of the minima and saddles of M_6 as functions of ρ_0, on an energy scale in which the energy of the global minimum is taken as −1.00 for all values of the range. Solid curves are energies of the minima, dashed curves are saddle energies. The order of each singular point is given in parentheses.

for ρ_0 below the critical value, one at the critical value, and one above.

The energy scales of Figure 11 reflect the fact that, if $\rho_0 = 0$, all pair interactions are equivalent and the energy of the system is just ϵ·(the number of pairs). If ρ_0 grows very large, only the nearest-neighbor pairs contribute to the total energy and the total energy for large ρ_0 is ϵ·(the number of nearest-neighbor pairs).

Considerable insight into the structure of the multidimensional potential comes from examining the content of Figure 13, whose upper panel shows the energies of all the stationary points of the M_6 surface as functions of ρ_0, on a scale that sets the energy of the global minimum to −1.00 for all values of the range. For $\rho_0 < 4.10$, the only minima are the regular octahedral and these are separated by simple, saddles where the structures are equilateral/triangular, right prisms, i.e. trigonal prisms. The motion carrying one octahedron into a geometrically equivalent, permutationally distinct octahedron is a twist of one triangular face against its opposite, around one of the four 3-fold rotation axes of the octahedron. The lower panel of Figure 13 shows some of the force constants of the trigonal prism (dashed curves; structure d of Figure 6) and of the capped, square-based pyramid (solid curves; structure b of Figure 6) as functions of ρ_0. For $\rho_0 < 1.95$, the M_6 trigonal prism has a single negative force constant, corresponding to the top of the reaction path between two octahedral minima. When ρ_0 exceeds 1.95, another force constant of the trigonal prism becomes negative, the force constant of the doubly degenerate E″ mode corresponding to a slewing motion of the triangular faces of the right prism, a motion that converts structure d of Figure 6 into structure c, the capped, square-based pyramid (CSBP). For $\rho_0 > 1.95$, the Murrell–Laidler theorem[44] correctly describes the trigonal prism: it is no longer a simple saddle and ceases to be the crest of the reaction path between two octahedra; its place is taken by the simple saddles of the lower-energy CSBP. The latter have only one negative force constant. For $\rho_0 > 4.10$, the CSBP is the saddle between two of the higher-energy, incomplete pentagonal bipyramid structures that belong to different octahedral "clocks." Other saddles appear at $\rho_0 = 3.54$ and at $\rho_0 = 4.10$, where the IPB saddle emerges from the fold catastrophe together with the IPB minimum.

This level of analysis is now altogether feasible. Of what use is it? There are at least two applications that we can now imagine. One is its application to testing approximate representations of potential surfaces for their robustness to small changes. If a surface shows a fresh fold appearing or apparently approaching, it would be wise to see how that surface changes if it is refined a little, particularly if the minimum and saddle or their progenitors would be important for a reaction path of interest. On the other hand if the surface shows only deep minima and strong saddles, with no incipient points of inflection, then the surface is likely to be robust toward small changes. Naturally this kind of diagnosis does not reveal major nonphysical misrepresentations of a model surface, such as one found for a surface for H_2CO, developed to represent the molecule near the equilibrium geometry of formaldehyde itself, which had a spurious global minimum corresponding to a linear H–H–C–O configuration with the hydrogens only 0.5 bohr apart.[58] A different, more global analysis must be used to find such artifacts.

A second application of systematic deformation of potential surfaces might come as a means to select the substances needed to give a material some desired set of properties. Many properties can be predicted from simulations, properties such as melting and freezing, surface melting, plasticity, and heat capacity. By carrying out such predictive simulations while systematically deforming the potential surface, it may be possible to use a two-step procedure to select the desired composition of a material. First, the parameters of the surface are varied until the desired characteristics appear in the simulation, and then the substances are selected that conform as closely as possible to those values of the parameters.

A third use, to understand how the shape of a multidimensional surface governs such dynamical properties as the propensity of a material to form a glass or a crystal, or to fold into a specific structure, will be discussed in the next section.

The possibilities of using surface deformation to find global minima and thereby to yield solutions to nonlinear optimizations problems are promising.[127] However a small caveat is necessary: in cases in which there are several minima rather close in energy (or in whatever the objective function of the optimization may be), the sequence of those minima may depend on the value of

the parameter or parameters used to deform the surface. In a model problem, the M_{14} cluster, it was found that the global minimum for very small values of ρ_0 was the second-lowest state for ρ_0 larger than 3.231.[135] This is in contrast to the seven- and 13-particle clusters, whose single deepest minima remain the global minima for all physically meaningful ρ_0.

B. Large Systems: Glass Formation

Systematic deformation of potential surfaces of large systems has not been carried out extensively yet. One exploratory study[116] of this topic illustrates how it may come to be used. This is in the context of glass vs crystal formation and of what characteristics of potential surfaces guide complex systems to specific shapes. The model for the study is the moderately large cluster $(KCl)_{32}$, far too large a system to have its potential mapped in detail yet small enough to tempt us to get and use information more specific than what we would have if we treated it as a bulk solid.

Pure, bulk alkali halides to not form glasses, although mixed salts do,[136,137] and there is at least one report of glassy films of alkali salts.[138] Simulations[112,116] of $(KCl)_{32}$ by a combination of molecular dynamics and quenching[14,15,139] showed, as described in section I.B.3, that there are four useful categories into which the catchment basins of this system can be classified, of which the highest in energy and the overwhelmingly dominant in number is the amorphous category. Most of the locally stable structures in this class are so disordered that they show virtually no short-range order, much less long-range order. This might lead one to expect such clusters to form glasses, in the sense of forming ensembles of the many kinds of disordered structures. Such ensembles form in simulations based on instantaneous quenching, the Stillinger–Weber procedure, in which no annealing dynamics are allowed. However if $(KCl)_{32}$ clusters are stimulated to go through a cooling and quenching process at a very fast but finite rate, e.g. even above 10^{12} K/s, the clusters find their way either to the global minimum, $4 \times 4 \times 4$ rocksalt structure or to a slightly defective rocksalt structure. Despite such high cooling rates, the system cannot be trapped in any of the many, many disordered structures. If the cooling rate is increased to 10^{13} [140] or 5×10^{13} K/s,[116] the system can be trapped in a disordered structure; this corresponds to taking roughly $(3N-6)k_B$ of energy from the cluster in 1/10 to 1/50 of a characteristic vibrational period, essentially instantaneous cooling. Consistent with this, is a report of simulations of $(NaCl)_{32}$ colliding with a liquid Ar reservoir, melting from the impact, and being quenched at a rate above 10^3 K/s by the evaporation of Ar atoms to form amorphous structures.[141] The potential surface of this system has a shape, therefore, that guides the cluster to its regular configuration, or very nearly so, unless the thermal energy can be removed in about 3 or fewer vibrational periods.[142]

What, then, would allow a simple binary system to form a glass? The most obvious characteristics are properties of the potential surface, inferred but for a long time, difficult to test and study,[110,143–145] but now becoming accessible: the barriers separating the local minima must be relatively high and that the "area" of the catchment basins corresponding to disordered

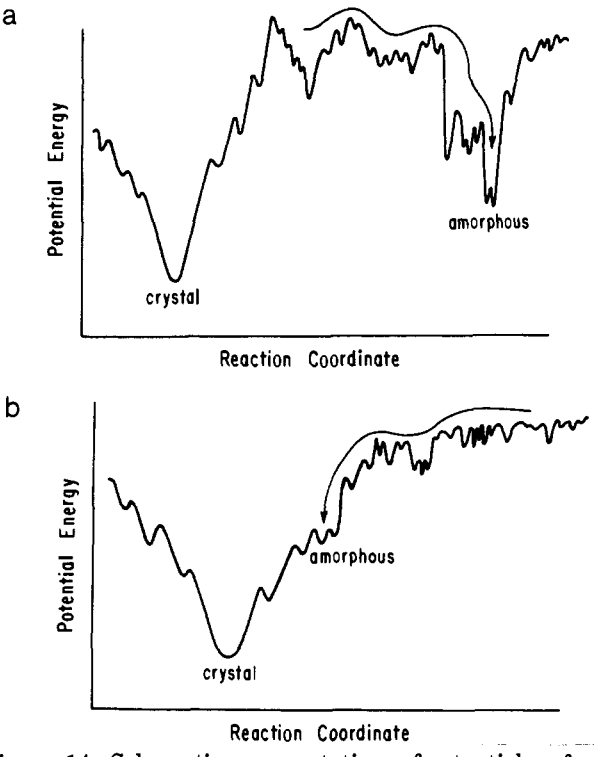

Figure 14. Schematic representations of potential surfaces for (a) a good glass-forming system, likely to be trapped in a high-energy minimum when cooled, and (b) a good crystal-forming system, likely to anneal to its global minimum when cooled at a finite rate.

structures must be large relative to that of the ordered structures. On the other hand a system will anneal to one of its lowest-energy structures if these are at the bottoms of very wide-mouthed basins, even if the side walls of these basins have many crannies, so long as the barriers between the minima of the crannies and the saddles connecting them to the large basins are low—and get lower—the deeper into the well the crannies are. Schematic representations of the potential surfaces for the two cases, a good glass-former and a good crystal-former, are shown in Figure 14.

The issue was investigated by making use of the fact that shortening the range of the outer part of the pair potential deepens the upper wells of the potential surface and increases their number.[116] The Coulomb interaction of the alkali halide pair potential is of course the longest-range potential possible, consistent with Gauss's theorem. By replacing the Coulomb potential with a shielded, Debye or Yukawa pair potential

$$V_{ij}(r) = A \exp(-r/\rho) + B \exp[-(\gamma_i + \gamma_j)r]q_iq_j/r$$

where r is the distance between ions i and j, q_i and q_j are the charges on the ions, ρ is a scale parameter independent of the particular ions, and γ_i and γ_j are tunable parameters characteristic of the ions. With $\gamma_i = \gamma_j = \gamma = 0.375$ Å^{-1}, i.e. a shielding length of 2.67 Å, the system could be trapped in disordered structures when the cooling rate was as low as 10^{11} K/s, still 2 orders of magnitude faster than the cooling rates reported by Suslick.[146] The further exploration of the relation between the structure of the potential surface and the capacity of a system to form a glass or to find a specific structure is clearly a fruitful direction for study.

IV. Closing Remarks

This very restricted discussion has examined the state of understanding of the multidimensional potential surfaces of systems for which it is possible to explore the shapes of the landscapes and, to some extent, to control them. We have not tried to review the vast literature concerned with construction of multidimensional potentials for small polyatomic molecules, but have selected a few examples that illustrated particular points. We have not treated the empirical potentials used to model large organic and metalloorganic systems, the potentials of "molecular mechanics", or the systems for which these potentials have been devised; the relation between such potentials and the subjects discussed here will surely emerge as the problem of glass vs crystal formation becomes more closely related to the problem of protein folding, and to the larger issue of what characteristics of a potential surface are responsible for guiding a system to a specific structure. We have tried to give a sense of some of the generalities of potential landscapes that govern reaction paths and rearrangement paths of molecules and clusters. And we have tried to point out a number of the open problems of the field, to tantalize the reader.

Acknowledgments

The authors wishes to thank his students and associates who have been responsible for so many of the results from our own work in this area, notably Thomas Beck, Paul Braier, Xiao-Yan Chang, Hai-Ping Cheng, Heidi Davis, R. J. Hinde, Julius Jellinek, John P. Rose, and David Wales. He would like to acknoeldge stimulating discussions of these topics with George Schatz and Frank Stillinger and to acknowledge also the support of the National Science Foundation and the Air Force Office of Scientific Research for those parts of the research described here that we carried out in our group at The University of Chicago.

References

(1) Murrell, J. N.; Carter, S.; Farantos, S. C.; Huxley, P.; Varandas, A. J. C. *Molecular Potential Energy Functions*; Wiley: New York, 1984.
(2) Hirst, D. M. *Potential Energy Surfaces*; Taylor and Francis: London, 1985.
(3) Dunning, T. H., Jr.; Harding, L. B. In *Theory of Chemical Reaction Dynamics*; Baer, M., Eds.; CRC Press: Boca Raton, FL, 1985.
(4) Truhlar, D. G.; Steckler, R.; Gordon, M. S. *Chem. Rev.* **1987**, *87*, 217.
(5) Schatz, G. C. *Revs. Mod. Phys.* **1989**, *61*, 669.
(6) Wales, D. J.; Berry, R. S. *J. Chem. Soc., Faraday Trans.* **1992**, *8*, 543.
(7) Beck, T.; Doll, J.; Freeman, D. *J. Chem. Phys.* **1989**, *90*, 5651.
(8) Hoare, M. R.; Pal, P. *Adv. Phys.* **1971**, *20*, 161.
(9) Hoare, M. R.; Pal, P. *J. Cryst. Growth* **1972**, *17*, 77.
(10) Hoare, M. R.; Pal, P. *Adv. Phys.* **1975**, *24*, 645.
(11) Hoare, M. In *The Glass Transition and the Nature of the Glassy State*; Goldstein, M. Simha, R., Eds.; Ann. N.Y. Acad. Sci.: New York, 1976.
(12) Hoare, M. R. *Adv. Chem. Phys.* **1979**, *40*, 49.
(13) Stillinger, F. H.; Weber, T. A. *J. Chem. Phys.* **1984**, *80*, 4434.
(14) Stillinger, F. H.; Weber, T. A. *Phys. Rev. A* **1982**, *25*, 978.
(15) Stillinger, F. H.; Weber, T. A. *Phys. Rev. A* **1983**, *28*, 2408.
(16) Press, W. H.; Flannery, B. P.; Teukolsky, S. A.; Vetterling, W. T. *Numerical Recipes*; Cambridge University Press: Cambridge, 1986.
(17) Uppenbrink, J.; Wales, D. J. *J. Chem. Soc., Faraday Trans.* **1991**, *87*, 215.
(18) Maranas, C. D.; Floudas, C. A. *J. Chem. Phys.* **1992**, *97*, 7667.
(19) Hoare, M. R.; Pal, P. *Nature* **1972**, *236*, 75.
(20) Hoare, M. R.; Pal, P. *Nature* **1972**, *230*, 5.
(21) Tsai, C. J.; Jordan, K. D. *J. Chem. Phys.* **1991**, *95*, 3850.
(22) Tsai, C. J.; Jordan, K. D. *J. Phys. Chem.* **1993**, *97*, 5208.
(23) McIver, J. W., Jr.; Komornicki, A. *J. Am. Chem. Soc.* **1972**, *94*, 2625.
(24) Komornicki, A.; McIver, J. W., Jr. *J. Am. Chem. Soc.* **1973**, *95*, 4512.
(25) Komornicki, A.; McIver, J. W., Jr. *J. Am. Chem. Soc.* **1974**, *96*, 5798.
(26) McIver, J. W. *Acc. Chem. Res.* **1974**, *7*, 72.
(27) Poppinger, H. *Chem. Phys. Lett.* **1975**, *35*, 550.
(28) Halgren, T. A.; Lipscomb, W. N. *Chem. Phys. Lett.* **1977**, *49*, 225.
(29) Mezey, P. G.; Peterson, M. R.; Csizmadia, I. G. *Can. J. Chem.* **1977**, *55*, 2941.
(30) Stephenson, L. M.; Brauman, J. I. *Acc. Chem. Res.* **1974**, *7*, 65.
(31) Slanina, *Z. Contemporary Theory of Chemical Isomerism*; D. Reidel: Dordrecht, 1986.
(32) Pancik, J. *Collect. Czech. Chem. Commun.* **1975**, *40*, 1112.
(33) Cerjan, C. J.; Miller, W. H. *J. Chem. Phys.* **1981**, *75*, 2800.
(34) Simons, J.; Jørgenson, P.; Taylor, H.; Ozment, J. *J. Phys. Chem.* **1983**, *87*, 2745.
(35) O'Neal, D.; Taylor, H.; Simons, J. *J. Phys. Chem.* **1984**, *88*, 1510.
(36) Banerjee, A.; Adams, N.; Simons, J. *J. Phys. Chem.* **1985**, *89*, 52.
(37) Baker, J. *J. Comput. Chem.* **1986**, *7*, 385.
(38) Baker, J. *J. Comput. Chem.* **1987**, *8*, 563.
(39) Shida, N.; Barbara, P. F.; Almlöf, J. E. *J. Chem. Phys.* **1989**, *91*, 4061.
(40) Wales, D. J. *J. Chem. Phys.* **1989**, *91*, 7002.
(41) Wales, D. J. *Chem. Phys. Lett.* **1990**, *166*, 419.
(42) Berry, R. S.; Davis, H. L.; Beck, T. L. *Chem. Phys. Lett.* **1988**, *147*, 13.
(43) Hinde, R. J.; Berry, R. S. *J. Chem. Phys.* **1993**, *99*, 2942.
(44) Murrell, J. N.; Laidler, K. J. *Trans. Faraday Soc.* **1968**, *64*, 371.
(45) Cheng, H.-P.; Li, X.; Whetten, R. L.; Berry, R. S. *Phys. Rev. A* **1992**, *46*, 79.
(46) Zauhar, R. J.; Morgan, R. S. *J. Comput. Chem.* **1990**, *11*, 603.
(47) Saxena, S.; Bhatt, P. C. P.; Prasad, V. C. *IEEE Trans. Comput.* **1990**, *39*, 400.
(48) Edelsbrunner, H. In *Algorithms in Combinatorial Geometry*; Brauer, W., Rozenberg, G., Saloma, A., Eds.; Springer-Verlag: New York, 1987.
(49) Csizmadia, I. G. In *Topological Features of Conformational Potential Energy Surfaces*; Mauruani, J., Serre, J., Eds.; Elsevier: Amsterdam, 1983.
(50) Mezey, P. G. *Potential Energy Hypersurfaces, Studies in Physical and Theoretical Chemistry*; Elsevier: Amsterdam, 1987.
(51) Aziz, R. A.; Chen, H. H. *J. Chem. Phys.* **1977**, *67*, 5719.
(52) Aziz, R. A. *Mol. Phys.* **1979**, *38*, 177.
(53) Aziz, R. A.; Slaman, M. *J. Mol. Phys.* **1986**, *58*, 679.
(54) Rittner, E. S. *J. Chem. Phys.* **1951**, *19*, 1030.
(55) Tosi, M. P.; Fumi, F. G. *J. Phys. Chem. Solids* **1964**, *25*, 45.
(56) Welch, D. O.; Lazareth, O. W.; Dienes, G. J.; Hatcher, R. D. *J. Chem. Phys.* **1976**, *64*, 835.
(57) Welch, D. O.; Lazareth, O. W.; Dienes, G. J.; Hatcher, R. D. *J. Chem. Phys.* **1978**, *68*, 2159.
(58) Davis, H. L.; Wales, D. J.; Berry, R. S. *J. Chem. Phys.* **1990**, *92*, 4473.
(59) Wales, D. J.; Berry, R. S. *J. Chem. Phys.* **1990**, *92*, 4283.
(60) Bartell, L. S. *Chem. Rev.* **1986**, *86*, 492.
(61) Martin, T. P. *Phys. Rep.* **1983**, *95*, 167.
(62) Bonačić-Koutecký, V.; Fantucci, P.; Koutecký, J. *Chem. Rev.* **1991**, *91*, 1035.
(63) Tomanek, D.; Mukherjee, S.; Bennemann, K. H. *Phys. Rev. B* **1983**, *28*, 665.
(64) Buttet, J. *Z. Phys. D* **1986**, *3*, 155.
(65) Andreoni, W. In *The Car-Parrinello Method and its Application to Microclusters*; Scoles, G., Ed.; North-Holland: Amsterdam, 1990.
(66) Li, S.; Bernstein, E. R. *J. Chem. Phys.* **1992**, *97*, 804.
(67) Wales, D. J.; Waterworth, M. C. *J. Chem. Soc., Faraday Trans.* **1992**, *88*, 3409.
(68) Wales, D. J. *Mol. Phys.* **1991**, *74*, 1.
(69) Müller, K.; Brown, L. D. *Theor. Chim. Acta (Berlin)* **1979**, *53*, 75.
(70) Johnson, B. F. G. *J. Chem. Soc., Chem. Commun.* **1986**, *1986*, 27.
(71) Sawada, S.; Sugano, S. *Z. Phys. D* **1989**, *12*, 189.
(72) Wales, D. J. *J. Chem. Soc., Faraday Trans.* **1992**, *88*, 653.
(73) Wales, D. J. *J. Chem. Soc., Faraday Trans.* **1993**, *89*, 1305.
(74) Richter, P. H.; Peitgen, H.-O. *Ber. Bunsen-Ges. Phys. Chem.* **1985**, *89*, 575.
(75) Martin, T. P. *Phys. Rev. B* **1973**, *7*, 3906.
(76) Martin, T. P. *J. Chem. Phys.* **1977**, *67*, 5207.
(77) Martin, T. P. *J. Chem. Phys.* **1978**, *69*, 2036.
(78) Martin, T. P. *J. Chem. Phys.* **1980**, *72*, 3506.
(79) Martin, T. P. *Physica B* **1984**, *127*, 214.
(80) Diefenbach, J.; Martin, T. P. *J. Chem. Phys.* **1985**, *83*, 4585.
(81) Phillips, N. G.; Conover, C. W. S.; Bloomfield, L. A. *J. Chem. Phys.* **1991**, *94*, 4980.
(82) Rose, J.; Berry, R. S. *J. Chem. Phys.* **1992**, *96*, 517.
(83) Etters, R. D.; Danilowicz, R. *J. Chem. Phys.* **1979**, *71*, 4767.
(84) Wales, D. J. *J. Chem. Soc., Faraday Trans.* **1990**, *86*, 3505.
(85) Doye, J. P. K.; Wales, D. J. *J. Chem. Soc., Faraday Trans.* **1992**, *88*, 3295.
(86) Li, S.; Johnson, R. L.; Murrell, J. N. *J. Chem. Soc., Faraday Trans.* **1992**, *88*, 1229.

(87) Raghavachari, K. *J. Chem. Phys.* **1986**, *84*, 5672.
(88) Raghavachari, K.; Rohlfing, C. M. *Chem. Phys. Lett.* **1988**, *143*, 428.
(89) Raghavachari, K.; Rohlfing, C. M. *J. Chem. Phys.* **1988**, *89*, 2219.
(90) Pacchioni, G.; Koutecký, J. *J. Chem. Phys.* **1986**, *84*, 3301.
(91) Pacchioni, G.; Koutecký, J. In *Electronic Structure of Small Carbon, Silicon and Germanium Clusters*; Plenum: New York, 1987.
(92) Tománek, D.; Schluter, M. A. *Phys. Rev. B* **1987**, *36*, 1208.
(93) Ballone, P.; Andreoni, W.; Car, R.; Parrinello, M. *Phys. Rev. Lett.* **1988**, *60*, 271.
(94) Patterson, C. H.; Messmer, R. P. *Phys. Rev. B* **1990**, *42*, 7530.
(95) Röthlisberger, U.; Andreoni, W. *Z. Phys. D* **1991**, *20*, 243.
(96) Röthlisberger, U.; Andreoni, W.; Giannozzi, P. *J. Chem. Phys.* **1992**, *96*, 1248.
(97) Houk, K. N.; Li, Y.; Evanseck, J. D. *Angew. Chem., Int. Ed. Engl.* **1992**, *31*, 682.
(98) Li, Y.; Houk, K. N. *J. Am. Chem. Soc.* **1993**, submitted for publication.
(99) Eichenauer, D.; LeRoy, R. J. *J. Chem. Phys.* **1988**, *88*, 2898.
(100) Kmetic, M. A.; LeRoy, R. J. *J. Chem. Phys.* **1991**, *95*, 6271.
(101) Gough, T. E.; Knight, D. G.; Scoles, G. *Chem. Phys. Lett.* **1983**, *97*, 155.
(102) Adams, J. E.; Stratt, R. M. *J. Chem. Phys.* **1990**, *93*, 1358.
(103) Fried, L. E.; Mukamel, S. *Phys. Rev. Lett.* **1991**, *66*, 2340.
(104) Ben-Horin, N.; Even, U.; Jortner, J. *Chem. Phys. Lett.* **1992**, *188*, 73.
(105) Hahn, M.; Whetten, R. L. *Phys. Rev. Lett.* **1988**, *61*, 1190.
(106) Raoult, B.; Farges, J.; DeFeraudy, M. F.; Torchet, G. *Phil. Mag. B* **1989**, *60*, 881.
(107) Stillinger, F. H.; Weber, T. A. *J. Chem. Phys.* **1985**, *83*, 4767.
(108) Labastie, P.; Whetten, R. L. *Phys. Rev. Lett.* **1990**, *65*, 1567.
(109) Tully, F. P.; Lee, Y. T.; Berry, R. S. *Chem. Phys. Lett.* **1971**, *9*, 80.
(110) Stillinger, F. H. *J. Chem. Phys.* **1988**, *88*, 7818.
(111) Bixon, M.; Jortner, J. *J. Chem. Phys.* **1989**, *91*, 1631.
(112) Rose, J. P.; Berry, R. S. *J. Chem. Phys.* **1993**, *98*, 3246.
(113) Grange, G.; Landers, R.; Mutaftschiev, B. *Surf. Sci.* **1976**, *54*, 445.
(114) Luo, J.; Landman, U.; Jortner, J. In *Isomerization and Melting of Small Alkali-Halide Clusters*; Jena, P., Rao, B. K., Khanna, S. N., Eds.; Plenum Press: New York, NY, 1987.
(115) Cheng, H.-P.; Berry, R. S. *Phys. Rev. A* **1992**, *45*, 7969.
(116) Rose, J.; Berry, R. S. *J. Chem. Phys.* **1993**, *98*, 3262.
(117) Valente, E. J.; Bartell, L. S. *J. Chem. Phys.* **1984**, *80*, 1458.
(118) Dibble, T. S.; Bartell, L. S. *J. Phys. Chem.* **1992**, *96*, 2317.
(119) Dibble, T. S.; Bartell, L. S. *J. Phys. Chem.* **1992**, *96*, 8603.
(120) Bartell, L. S.; Harsanyi, L.; Valente, E. J. *J. Phys. Chem.* **1989**, *93*, 6201.
(121) Bartell, L. S.; Chen, J. *J. Phys. Chem.* **1992**, *96*, 8801.
(122) Bartell, L. S.; Xu, S. *J. Phys. Chem.* **1991**, *95*, 8939.
(123) Berry, R. S.; Beck, T. L.; Davis, H. L.; Jellinek, J. In *Solid-Liquid Phase Behavior in Microclusters*; Prigogine, I., Rice, S. A., Eds.; John Wiley and Sons: New York, 1988.
(124) Berry, R. S. *J. Chem. Soc., Faraday Trans.* **1990**, *86*, 2343.
(125) Raynerd, G.; Tatlock, G. J.; Venables, J. A. *Acta Crystallogr.* **1982**, *B38*, 1896.
(126) Pawley, G. S.; Dove, M. T. *Chem. Phys. Lett.* **1983**, *99*, 45.
(127) Stillinger, F. H.; Weber, T. A. *J. Stat. Phys.* **1988**, *52*, 1429.
(128) Stillinger, F. H.; Stillinger, D. K. *J. Chem. Phys.* **1990**, *93*, 6106.
(129) Kirkpatrick, S.; Gelatt, C. D.; Vecchi, M. P. *Science* **1983**, *220*, 671.
(130) Piela, L.; Kostrowicki, J.; Scheraga, H. A. *J. Phys. Chem.* **1989**, *93*, 3339.
(131) Kostrowicki, J.; Piela, L.; Cherayil, B. J.; Scheraga, H. A. *J. Phys. Chem.* **1991**, *95*, 4113.
(132) Pillardy, J.; Olszewski, K. A.; Piela, L. *J. Phys. Chem.* **1992**, *96*, 4337.
(133) Braier, P. A.; Berry, R. W.; Wales, D. J. *J. Chem. Phys.* **1990**, *93*, 8745.
(134) Head-Gordon, T.; Stillinger, F. H.; Arrecis, J. *Proc. Nat. Acad. Sci. U.S.A.* **1991**, *88*, 11076.
(135) Chang, X.-y. *J. Chem. Phys.* **1992**, *97*, 3573.
(136) Kadono, K.; Mitani, K.; Kinugawa, K.; Tanaka, H. *J. Non-Cryst. Solids* **1990**, *122*, 214.
(137) Kinugawa, K. *J. Chem. Phys.* **1992**, *97*, 8581.
(138) Consani, K.; Devlin, J. P.; Ray, A.; Farrar, H., III; Wilson, E. W., Jr. *J. Chem. Phys.* **1981**, *74*, 4774.
(139) Stillinger, F. H.; Weber, T. A. *Kinam* **1981**, *3*, *Serie A*, 159.
(140) Amini, M.; Hockney, R. W. *J. Non-Cryst. Sol.* **1979**, *31*, 447.
(141) Cheng, H.-P.; Landman, U. *Science* **1993**, *260*, 1304.
(142) Huber, K. P.; Herzberg, G. *Constants of Diatomic Molecules*; Van Nostrand Reinhold: New York, 1979.
(143) Goldstein, M. *J. Chem. Phys.* **1969**, *51*, 3728.
(144) Goldstein, M. *J. Chem. Phys.* **1976**, *64*, 4767.
(145) Goldstein, M. *J. Chem. Phys.* **1977**, *67*, 2246.
(146) Suslick, K. *Science* **1990**, *247*, 1439.